

When to repeat a biomarker test? Decomposing sources of variation from conditionally repeated measurements

Supun Manathunga¹, Mart P. Janssen², Yu Luo³, W. Alton Russell^{1,4}, and Mart Pothast²

¹Experimental Medicine, McGill University, Montreal, Canada

²Transfusion Technology Assessment, Sanquin Research, Amsterdam, Netherlands

³Department of Mathematics, King's College, London, United Kingdom

⁴Epidemiology, Biostatistics and Occupational Health, McGill University, Montreal, Canada

February 17, 2026

Abstract

Repeating an imperfect biomarker test based on an initial result can introduce bias and influence misclassification risk. For example, in some blood donation settings, blood donors' hemoglobin is remeasured when the initial measurement falls below a minimum threshold for donor eligibility. This paper explores methods that use data resulting from processes with conditionally repeated biomarker measurement to decompose the variation in observed measurements of a continuous biomarker into population variability and variability arising from the measurement procedure. We present two frequentist approaches with analytical solutions, but these approaches perform poorly in a dataset of conditionally repeated blood donor hemoglobin measurements where normality assumptions are not met. We then develop a Bayesian hierarchical framework that allows for different distributional assumptions, which we apply to the blood donor hemoglobin dataset. Using a Bayesian hierarchical model that assumes normally distributed population hemoglobin and heavy tailed t -distributed measurement variation, we estimate that measurement variation is responsible for 22% of the total variance for females and 25% for males in point-of-care hemoglobin measures, with population standard deviations of 1.07 g/dL for female donors and 1.28 g/dL for male donors. Our Bayesian framework can use data resulting from any clinical process with conditionally repeated biomarker measurement to estimate individuals' misclassification risk after one or more noisy continuous measurements and inform evidence-based conditional retesting decision rules.

Keywords: *Measurement variation, Repeated measurements, Bayesian modelling, hierarchical models, Blood donation*

1 Introduction

Biomarker levels, such as blood pressure, blood glucose, cholesterol, C-reactive protein, and hemoglobin, play a prominent role in modern medicine. Diagnosis and treatment decisions often involve dichotomizing a continuous biomarker to classify an individual as positive for a condition (e.g., diagnose diabetes based on hemoglobin A1C) or as indicated for an intervention (e.g., transfuse red cells based on hemoglobin). When using imperfect tests, repeating a biomarker measurement can reduce measurement uncertainty and lower the risk of misclassification (false positives or false negatives). Because measurements close to a decision threshold are more likely to produce misclassifications, clinicians often observe an initial measurement before deciding whether to collect an additional measurement. Repeating critical values in clinical chemistry laboratories is also common, but its added value is uncertain [1, 2, 3]. However, the specific re-testing strategy (when a measurement is repeated and how measurements inform further decisions) may lead to a “sequential testing bias” similar to what is described for clinical trials[4, 5].

This paper focuses on the case of measurement of hemoglobin (Hb) prior to blood donation. Low Hb in blood donors can indicate anemia, which can develop donation-associated iron deficiency [6, 7]. Thus, as recommended by the WHO[6], most countries screen donors to ensure that Hb levels exceed a minimum threshold before blood donation, often different for male and female donors. Failing the pre-donation Hb test is the single most common reason for on-site deferral of blood donation[8]. Low Hb deferrals protect donor health by preventing the exacerbation of iron deficiency and anemia. However, deferrals lead to the loss of a potential donation, waste blood establishment resources, and are inconvenient for donors who traveled to a donation center. Low Hb deferrals are also donor dissatisfiers, reducing the likelihood of return for future donations[9, 10, 11].

Pre-donation Hb is usually measured in a fingerstick capillary sample using a point-of-care device. Prior work has found substantial variation in fingerstick Hb measurements. Fingerstick samples have more pre-analytical “drop-to-drop” variation than venous blood draws[12, 13, 14], leading to limited sensitivity and specificity when used to diagnose anemia[15]. Therefore, many low Hb deferrals likely result from erroneous low Hb measurements and may be unnecessary[16]. Several blood establishments reported to repeat a Hb fingerstick measurement that is below the threshold for donation[17].

Wasteful “false positive” low hemoglobin deferrals must be balanced against “false negatives,” when a donor is classified as having sufficient Hb due to an erroneously high Hb measurement. Risk of false negatives must be minimized to avoid removing iron-containing blood from donors with insufficiently recovered Hb or iron deficiency anemia from another cause. The risk of false positives and negatives depends on both the measurement uncertainty distribution as well as the distribution of Hb levels in blood donor populations.

The questions that arise are: when is it sensible to repeat a capillary Hb measurement? And how should we interpret these repeated measurements? From the blood service perspective, it is tempting to stop when the measurement is above the threshold, using the maximum of all measurements. It was

shown by Chung et al. (2017)[18] that such a testing strategy may lead to biases in the recorded Hb levels, and Pothast et al. (2025)[19] showed this strategy skews the distribution of recorded Hb levels. Quantifying the sources of variation can inform whether a Hb measurement is potentially misclassified and whether a repeat measurement is applicable.

In this paper, we investigate several methods to determine the measurement variation from datasets in which repeated measurements are conditionally observed and apply these methods to quantifying measurement variability in blood donor fingerstick Hb measurements. In section 2 we provide background information and mathematical notation for the problem of conditionally repeated measurements. In section 3 we describe the dataset at our disposal. Then in section 4 we derive two frequentist methods to decompose the sources of variation under normality assumptions. After observing that this assumption is not met in our data and studying how this can affect our estimates, we resort to Bayesian methods in section 5, where we model other distributions explicitly and we show how Hb measurements in our data can be best represented. Finally, in section 6 we discuss our results and how they can aid in interpreting repeated (Hb) measurements and other clinical applications.

2 Background

2.1 Notation and terminology

We assume that the total variation of a biomarker level measured across a population of individuals is coming from two sources: (1) the variation in the population of the “true” level (the “between persons” variation) and (2) the variation coming from the measurement, which is defined as the variation between repeated measurements of the same individual at a single point in time. Another source of variation is the variation of the “true” level *within* an individual over time, but here we consider that to be part of the population variation[20].

We define the true biomarker level for an individual i as T_i , ignoring temporal variability within individuals. T_i is drawn from the population distribution with mean μ and noise ϵ_{pop} , i.e., $T_i = \mu + \epsilon_{\text{pop}}$. A biomarker measurement x_i with noise ϵ_{meas} can be written as:

$$x_i = T_i + \epsilon_{\text{meas}} = \mu + \epsilon_{\text{pop}} + \epsilon_{\text{meas}} \quad (1)$$

Assuming independent ϵ_{pop} and ϵ_{meas} , the distribution of biomarker measurements is the convolution of population variability and measurement error:

$$f_X(x) = (f_{\text{pop}} * g_{\text{meas}})(x) = \int f_{\text{pop}}(t)g_{\text{meas}}(x - t)dt \quad (2)$$

where $f_{\text{pop}}(\cdot)$ is the probability density function of biomarker levels in the population and $g_{\text{meas}}(\cdot)$ the probability density function of a single measurement.

2.2 Non-conditionally repeated measurements

The measurement variability in a noisy test can be estimated when repeated measurements are available for the same individuals. For an individual i whose true biomarker level is T_i , biomarker measurement $j \in \{1, \dots, J\}$ can be written as:

$$x_{i,j} = T_i + \epsilon_{i,j}, \quad (3)$$

where $\epsilon_{i,j}$ denote random measurement error. With two measurements per individual, we have:

$$\begin{aligned} x_{i,1} &= T_i + \epsilon_{i,1} \\ x_{i,2} &= T_i + \epsilon_{i,2}. \end{aligned} \quad (4)$$

and the difference between the two measurements:

$$\Delta_i = x_{i,1} - x_{i,2} = \epsilon_{i,1} - \epsilon_{i,2} \quad (5)$$

If we assume that $\epsilon_{i,j}$ has mean 0, variance σ_{meas}^2 , and is independent of T_i and j , then

$$\begin{aligned} \text{Var}(\Delta_i) &= \text{Var}(\epsilon_{i,1}) + \text{Var}(\epsilon_{i,2}) = 2\sigma_{\text{meas}}^2 \\ \sigma_{\text{meas}}^2 &= \text{Var}(\Delta_i)/2. \end{aligned} \quad (6)$$

Thus, by estimating the variance of the difference between two repeated measurements, one can estimate σ_{meas}^2 , the variance of the measurement procedure.

2.3 Conditionally repeated measurements

We now consider the case when the decision to take a second measurement depends on the result of a first measurement; for example, when a second fingerstick Hb is only recorded if a blood donor's first fingerstick Hb falls below the donor eligibility threshold. Figure 2 shows an example with simulated data. In such settings, pairs of measurements are conditionally observed and eq. (6) no longer provides an unbiased estimate of the measurement variance σ_{meas}^2 .

Let c denote a threshold below which the first measurement is repeated. If we only observe $\Delta_i = x_{i,1} - x_{i,2}$ when $x_{i,1} < c$, this induces selection on the measurement error $\epsilon_{i,1}$ while $\epsilon_{i,2}$ remains unbiased. Naively applying eq. (6) will result in:

$$\hat{\sigma}_{\text{meas}}^2 = \frac{\text{Var}(\Delta_i \mid x_{i,1} < c)}{2} = \frac{\text{Var}(\epsilon_{i,1} \mid x_{i,1} < c) + \sigma_{\text{meas}}^2}{2}.$$

Because conditional retesting reduced the observed variability in $x_{i,1}$, $\text{Var}(\Delta_i \mid x_{i,1} < c) < 2\sigma_{\text{meas}}^2$ and $\hat{\sigma}_{\text{meas}}^2$ will be a biased underestimation of σ_{meas}^2 .

When the population biomarker levels and measurement noise are independent and normally distributed, this bias can be explicitly expressed. Let

$$T_i \sim \mathcal{N}(\mu, \sigma_{\text{pop}}^2), \quad (7)$$

$$\epsilon_{i,j} \sim \mathcal{N}(0, \sigma_{\text{meas}}^2). \quad (8)$$

The marginal distribution of a biomarker measurement $x_{i,j}$ is then normal with mean μ and total variance:

$$\sigma_{\text{total}}^2 = \sigma_{\text{pop}}^2 + \sigma_{\text{meas}}^2. \quad (9)$$

Let

$$\alpha = \frac{c - \mu}{\sigma_{\text{total}}} \quad \text{and} \quad \lambda = \frac{\phi(\alpha)}{\Phi(\alpha)}, \quad (10)$$

where ϕ and Φ denote the standard normal density and cumulative distribution functions, respectively. Then, from Johnson (1994)[21],

$$\text{Var}(\epsilon_{i,1} \mid x_{i,1} < c) = \sigma_{\text{meas}}^2 \left[1 - \frac{\sigma_{\text{meas}}^2}{\sigma_{\text{total}}^2} (\alpha\lambda + \lambda^2) \right], \quad (11)$$

and therefore

$$\text{Var}(\Delta_i \mid x_{i,1} < c) = 2\sigma_{\text{meas}}^2 - \frac{\sigma_{\text{meas}}^4}{\sigma_{\text{total}}^2} (\alpha\lambda + \lambda^2). \quad (12)$$

Therefore, the naive estimator $\hat{\sigma}_{\text{meas}}^2 = \text{Var}(\Delta_i \mid x_{i,1} < c)/2$ underestimates σ_{meas}^2 by $\frac{\sigma_{\text{meas}}^4}{2\sigma_{\text{total}}^2} (\alpha\lambda + \lambda^2)$. The magnitude of the bias depends on the threshold c through α . Thus, normality assumptions enable explicit correction for this truncation via properties of the conditional normal distribution. We compare bias curves obtained from this theoretical result to simulated data in fig. B1.

3 Blood donor Hb data

Following sections will assess methods using pre-donation fingerstick Hb screening data from Vitalant, one of the largest blood collectors in the United States. Our dataset includes visits between January 2017 and October 2022. The full dataset contains 2,582,402 unique donors and 9,099,136 donation visits, of which 6,528,084 had a recorded pre-donation fingerstick Hb measurement.

We restricted the analysis to only first visits of any type of intended donation, resulting in 1,863,159 visits from unique donors. We further selected only same-day repeated measurements to isolate measurement variability from longer-term biological variation. The data were stratified by sex, with donation eligibility thresholds of 13 g/dL for males and 12.5 g/dL for females. Among males, 18,173 of 849,469 (2.1%) initial Hb measurements were below the eligibility threshold, prompting a second measurement for 17,195 visits (94.6%). Among females, 123,379 of 1,013,690 (12.2%) initial Hb

measurements fell below the threshold, prompting a second measurement for 114,840 visits (93.1%). A flow chart of the data selection process is provided in fig. A1. The distribution of initial Hb measurements and the relationship between initial and repeat measurements are shown in fig. 1.

4 Frequentist approaches

In this section, we derive and evaluate two frequentist methods for deriving the measurement and population variance from conditionally repeated measurements, correcting for the bias induced by naively applying eq. (6). Both methods assume T_i and $\epsilon_{i,j}$ are normally distributed. Therefore, repeated measurements follow a multivariate normal distribution with J dimensions where J is the number of repeated measurements per individual. When $J = 2$, fully observed measurement pairs $(x_{i,1}, x_{i,2})$ follow a bivariate normal distribution with mean (μ, μ) and covariance matrix

$$\text{Cov}(x_{i,1}, x_{i,2}) = \begin{pmatrix} \sigma_{\text{total}}^2 & \rho\sigma_{\text{total}}^2 \\ \rho\sigma_{\text{total}}^2 & \sigma_{\text{total}}^2 \end{pmatrix}. \quad (13)$$

The total variance is given by eq. (9) and the correlation coefficient between $x_{i,1}$ and $x_{i,2}$ is

$$\rho = \frac{\sigma_{\text{pop}}^2}{\sigma_{\text{total}}^2}. \quad (14)$$

Note that estimating σ_{pop}^2 and σ_{meas}^2 is equivalent to estimating ρ and σ_{total}^2 . Because $x_{i,1}$ is observed for all N individuals, we can estimate the mean true biomarker level μ and total variance σ_{tot}^2 without bias as:

$$\hat{\mu} = \frac{1}{N} \sum_{i=1}^N x_{i,1} \quad (15)$$

$$\hat{\sigma}_{\text{total}}^2 = \frac{\sum_{i=1}^N (x_{i,1} - \hat{\mu})^2}{N - 1}. \quad (16)$$

4.1 Conditional expectation method

When the second measurement is only observed when $x_1 < c$, the conditional means of paired measurements are shifted downward relative to μ according to the truncation factor λ from eq. (10):

$$E[x_1 | x_1 < c] = \mu - \sigma_{\text{total}}\lambda, \quad (17)$$

$$E[x_2 | x_1 < c] = \mu - \rho\sigma_{\text{total}}\lambda. \quad (18)$$

The correlation coefficient ρ is identifiable from the difference between the two conditional means:

$$\rho = 1 - \frac{E[x_2 | x_1 < c] - E[x_1 | x_1 < c]}{\sigma_{\text{total}}\lambda}. \quad (19)$$

In practice, $\hat{\rho}_{\text{CE}}$ is obtained using eq. (19) by replacing the conditional expectations with the sample means of the truncated paired observations and the sample mean and variance as in eq. (16).

Table 1: Comparison of true and estimated variance parameters across methods for simulated data, with estimates reported as mean \pm SD of 1000 simulated datasets with $N = 10000$.

Method	True σ_{pop}^2	Est. $\sigma_{\text{pop}}^2 \pm \text{SD}$	True σ_{meas}^2	Est. $\sigma_{\text{meas}}^2 \pm \text{SD}$
Conditional expectation	1.00	1.00 \pm 0.04	0.64	0.64 \pm 0.03
Maximum likelihood	1.00	1.00 \pm 0.02	0.64	0.64 \pm 0.02

4.2 Maximum likelihood estimation

The correlation coefficient ρ can also be estimated through maximum likelihood. Assuming a bivariate normal distribution, the log-likelihood of the data under truncation is

$$\begin{aligned} \mathcal{L}(\mu, \sigma_{\text{total}}, \rho) = & \sum_{i=1}^n \log f_{2D}(x_{i,1}, x_{i,2} | \mu, \sigma_{\text{total}}, \rho) \\ & + n \log P(x_{i,1} < c), \end{aligned} \quad (20)$$

where f_{2D} represents the density function of the bivariate normal distribution and $P(x_1 < c)$ can be evaluated using the cumulative distribution function of the univariate normal distribution. Setting the derivative with respect to ρ equal to 0 gives us:

$$\begin{aligned} \frac{d\mathcal{L}}{d\rho} = & \rho^3 - (1 + \rho^2) \frac{1}{N} \sum_i x'_{i,1} x'_{i,2} \\ & + \rho \left(\frac{1}{N} \sum_i (x'^2_{i,1} + x'^2_{i,2}) - 1 \right) = 0, \end{aligned} \quad (21)$$

where $x'_{i,j} = \frac{x_{i,j} - \mu}{\sigma_{\text{total}}}$ and N is the number of paired observations. In practice, $\hat{\rho}_{\text{MLE}}$ is obtained by setting $\mu = \hat{\mu}$ and $\sigma_{\text{total}} = \hat{\sigma}_{\text{total}}$ from eq. (16).

Note that the cutoff c does not appear in $\frac{d\mathcal{L}}{d\rho}$. Therefore, unlike $\hat{\rho}_{\text{CE}}$, estimating ρ using maximum likelihood does not require knowledge of the retesting cutoff.

4.3 Frequentist approaches in simulated data

We simulated Hb measurements with the conditional rechecking under normality assumptions. Figure 2 shows simulated data with population mean $\mu = 15 \text{ g/dL}$, population standard deviation $\sigma_{\text{pop}} = 1 \text{ g/dL}$, and measurement standard deviation $\sigma_{\text{meas}} = 0.8 \text{ g/dL}$, and a retesting cutoff $c = 13 \text{ g/dL}$.

For these parameters, the correlation between the initial and the repeated measurement, if every measurement was unconditionally repeated is $\rho = \frac{1^2}{1^2 + 0.8^2} \approx 0.61$. We estimate $\hat{\rho}$ from the conditionally repeated measurement data by the conditional expectation method (eq. (19)) and the maximum likelihood method (eq. (21)) on 1000 simulated datasets with $N = 10000$ initial measurements. Both methods successfully recover the true ρ (table 1). Similar results were found using various parameters for μ , σ_{pop} , σ_{meas} , and c (data not shown).

Conditionally repeated measurements with additional dependencies

In the previous simulation, the only condition for repeating a measurement was the initial measurement being less than the cutoff value, so

$$p = \begin{cases} 1, & \text{if } x_1 < c \\ 0, & \text{otherwise} \end{cases} \quad (22)$$

where p is the probability of observing a repeat measurement. But more complex conditional retesting processes are possible. For example, initial values that are closer to the cutoff might be more likely to be repeated. To assess our methods under such conditions, we simulated data in which an individual was conditionally retested with the following probability:

$$p = \begin{cases} e^{-r(c-x_1)}, & \text{if } x_1 < c \\ 0, & \text{otherwise.} \end{cases} \quad (23)$$

A larger rate parameter r means that individuals with an initial measurement far from the threshold are less likely to be retested, as visualized in fig. B2. We observed substantial bias in $\hat{\rho}_{CE}$, for larger values of r , but $\hat{\rho}_{MLE}$ remained unbiased across simulations (fig. 3). This result is expected since $\hat{\rho}_{CE}$ depends on the cutoff c , but $\hat{\rho}_{MLE}$ does not. Thus, our simulations show that $\hat{\rho}_{MLE}$ is more robust to the specific conditions governing which individuals are retested.

4.4 Frequentist approaches in real data

Using the full dataset described in section 3, we estimated the measurement error variance and population variance using the conditional expectation and the maximum likelihood methods. Uncertainty was estimated using 1,000 bootstrap samples.

The estimates obtained using the conditional expectation method and the maximum likelihood method are summarized in table 2 and the distributions of the estimates by each method are depicted in fig. 4. We observed a significant difference in estimates for the population variance, measurement error variance across the two methods and across males and females for each method. The maximum likelihood method should not be susceptible to additional conditional dependencies (as studied in section 4.3), but what is remarkable is that the measurement error variance is significantly different for males ($\hat{\sigma}_{meas}^2 = 0.61 \pm 0.03 \text{ g/dL}$) and females ($\hat{\sigma}_{meas}^2 = 0.34 \pm 0.01 \text{ g/dL}$). This leads us to believe that there are additional systematic uncertainties for this method, which we will investigate below.

4.5 Limitations of frequentist approaches

The conditional expectation method and the maximum likelihood method both rely on the assumption that measurement errors are normally distributed. In the presence of outliers (heavy tails), the variance decomposition and the correlation relationship in eq. (14) no longer hold, and the resulting estimates can be biased.

Table 2: Estimated population variance, measurement error variance reported as mean \pm SD by method and sex.

Method	Sex	$\hat{\sigma}_{\text{pop}}^2$	$\hat{\sigma}_{\text{meas}}^2$
Conditional expectation	Female	1.05 \pm 0.01	0.38 \pm 0.01
Conditional expectation	Male	1.57 \pm 0.01	0.52 \pm 0.02
Maximum likelihood	Female	1.10 \pm 0.01	0.34 \pm 0.01
Maximum likelihood	Male	1.48 \pm 0.02	0.61 \pm 0.03

To study the effect of outliers, we simulated conditionally repeated Hb levels, similar to section 4.3, but with a t -distributed measurement error with different degrees of freedom df . The scale parameter of the t distribution is denoted by s ; the corresponding variance then equals $s^2 \frac{df}{df-2}$ for $df > 2$. Therefore, the estimated measurement uncertainty, using our naive approaches from before, $\hat{\sigma}_{\text{meas}}$ should be multiplied by $\sqrt{\frac{df}{df-2}}$ to compare with s .

The difference between the estimated $\hat{\sigma}_{\text{meas}}$ using the maximum likelihood method (the conditional expectation method behaves similarly) and the simulated value is shown in fig. 5. For large df the scenario matches the normal-error case and bias is negligible. However, for $df < 10$ both methods overestimates $\hat{\sigma}_{\text{meas}}$ by more than 5%.

Extending the closed-form estimates for ρ and σ_{meas} to non-normal distributional assumptions is challenging. Instead, section 5 proposes a Bayesian hierarchical modelling framework to decompose measurement and population variability from conditionally repeated measurements under flexible distributional assumptions.

5 Bayesian approach

Bayesian hierarchical models have gained popularity in cases when repeated measurements are conditionally dependent. In such settings, hierarchical formulations allow the decomposition of variability into measurement-level noise, unit-level heterogeneity, and higher-order contextual dependence. There is a rich literature demonstrating the Bayesian hierarchical approaches in capturing complex dependence structures. For example, Gustafson (2003)[22] provided one of the foundational treatments of Bayesian hierarchical modelling for measurement error and misclassification, demonstrating how hierarchical structures can explicitly represent uncertainty in both exposure assessment and outcome processes. Greenland (2005)[23] incorporated Bayesian hierarchical modelling within a multiple-bias framework to simultaneously adjust for several key sources of bias, including exposure misclassification, selection bias, and confounding, in an observational study of childhood leukemia. Similarly, Luo et al. (2018)[24] employed a hierarchical Bayesian framework to estimate the prevalence of attention-deficit/hyperactivity disorder (ADHD), accounting fully for the uncertainty, variability and spatial dependence for the estimate. Therefore, in this section, we will apply the hierarchical modelling framework to decompose the variations arising from conditionally repeated measurements of a con-

tinuous biomarker.

5.1 Bayesian model structure

We model biomarker measurements using a two-level measurement error framework. As before, an individual i has an unobserved true biomarker level T_i at the time of a visit. We assume that

$$T_i \sim f_{\text{pop}}(\cdot | \theta_{\text{pop}}), \quad (24)$$

where f_{pop} denotes the population distribution of true biomarker level with parameters θ_{pop} .

An observed measurement $x_{i,j}$ is a noisy observation of T_i , affected by measurement error with parameters θ_{meas}

$$x_{i,j} | T_i \sim g_{\text{meas}}(\cdot | T_i, \theta_{\text{meas}}). \quad (25)$$

A pair of measurements on the same individual $x_{i,1}$ and $x_{i,2}$ have the same underlying true measure T_i , so any within-pair variability is attributable to the measurement process, as shown graphically in fig. 6. This allows for identification of the measurement error distribution.

The following sections consider hierarchical models with four sets of distributional assumptions for the latent true biomarker level T_i and the measurement error process ϵ_{meas} (shown in detail in fig. B3):

- a) **Model a** : Normal true biomarker level with normal measurement error
- b) **Model b** : Normal true biomarker level with Student- t measurement error
- c) **Model c** : Normal true biomarker level with mixture of normal measurement error
- d) **Model d** : Skew-normal true biomarker level with Student- t measurement error

5.2 Model estimation in simulated data

We used simulations to assess whether our hierarchical modelling framework could correctly estimate underlying parameters when the distribution of the data generating process is known. First, we simulated four datasets corresponding to the distributions of models a-d with parameter values given in table C1. Then, we fit the corresponding Bayesian model to each simulated dataset using Markov chain Monte Carlo (MCMC). Models used weakly informative priors for top-level parameters such that the prior predictive distribution of observed Hb measurements lay within physiologically plausible ranges, with most of the mass between 12 and 18 g/dL (table C2)[25]. We computed posterior summaries for all parameters.

Across simulated datasets, the posterior distributions concentrate around the true values used to generate the data. In particular, the true parameter values fall within the 95% credible intervals for the estimated parameters, indicating that the proposed likelihood and prior specification can recover the data-generating parameters under the study design. Posterior means and 95% credible intervals are reported in table C3.

5.3 Model selection in simulated data

Next, we assessed whether a model selection procedure would correctly identify the model that corresponds to the data-generating process underlying our four simulated datasets. Our model selection process used 5-fold cross-validation to compare candidate models and selected the model with the largest marginal log pointwise predictive density (marginal LPPD). Following standard K -fold cross-validation, the data are partitioned into K disjoint folds. For each fold, the model is fit to the remaining $K - 1$ folds and evaluated on the held-out data. For a Bayesian model with parameters θ , predictive performance on a validation set is summarized by the LPPD, which integrates over posterior uncertainty in the parameters[26].

For a validation fold containing n observations $\{x_i\}_{i=1}^n$, the LPPD is defined as

$$\text{LPPD} = \sum_{i=1}^n \log \left(\int p(x_i | \theta) p_{\text{post}}(\theta) d\theta \right), \quad (26)$$

where $p_{\text{post}}(\theta)$ denotes the posterior distribution of θ obtained from the training data.

Our generative model includes individual-specific latent true Hb values that are not shared across training and validation folds. Consequently, predictive evaluation must integrate over these latent variables rather than conditioning on their posterior values from the training fit. We therefore compute a marginal predictive density for the validation data by integrating out the latent true Hb values, yielding predictions that are unconditional on any specific latent state and appropriate for new individuals.

For a validation set with n observations, the marginal LPPD (mLPPD) is given by

$$\text{mLPPD} = \sum_{i=1}^n \log \left(\iint p(x_i | T_i, \theta) p(T_i | \theta) p_{\text{post}}(\theta) dT_i d\theta \right) \quad (27)$$

where $\theta = (\theta_{\text{pop}}, \theta_{\text{meas}})$. We approximate the outer integral using S posterior draws $\{\theta^{(s)}\}_{s=1}^S$ obtained from the training-set fit. For each fixed $\theta^{(s)}$, the inner integral over the latent true Hb T_i is approximated using R Monte Carlo draws $\{x_i^{(s,r)}\}_{r=1}^R \sim p(x_i | \theta^{(s)})$. The resulting computed marginal LPPD (cLPPD) estimator is

$$\text{cLPPD} = \sum_{i=1}^n \log \left(\frac{1}{S} \sum_{s=1}^S \hat{p}(x_i | \theta^{(s)}) \right), \quad (28)$$

where

$$\hat{p}(x_i | \theta^{(s)}) = \frac{1}{R} \sum_{r=1}^R p(x_i | T_i^{(s,r)}, \theta^{(s)}).$$

For each true model, we computed 5-fold CV cLPPD across all fitted models and compared their total scores (table C4). As shown in fig. 7, the model corresponding to the true data generation process has the highest cLPPD for three of four datasets and is within a negligible margin of the best score for the fourth, indicating that cLPPD can reliably recover the correct generative model

Table 3: Paired (foldwise) differences between **Model d** and other models. Positive values indicate better performance for **Model d**.

Comparison	Mean ($cLPPD_{\text{other}} - cLPPD_{\text{Model d}}$)	SD(diff)	SE(diff)
Model b – Model d	–2.35	9.52	4.26
Model c – Model d	–7.59	15.54	6.95
Model a – Model d	–40.83	17.82	7.97

across simulated settings. When competing models are close, the differences in $cLPPD$ are small and the ranking is effectively indistinguishable, suggesting that the models are practically equivalent for prediction in those scenarios.

5.4 Model selection in real data

We now apply our model selection procedure to real data (section 3). To reduce computation time, we analyzed a random sample of 10,000 male and 10,000 female donors from the filtered dataset. We computed 5-fold $cLPPD$ for candidate models **a-d**; per-fold values are summarized in table C5.

The skew-t model (**Model d**) achieved the largest mean $cLPPD$, but its advantage over the normal-t model (**Model b**) was small (mean difference = 2.35, SE = 4.26), and the difference relative to the mixture model (**Model c**) was similarly modest (mean difference = 7.59, SE = 6.95) (table 3). In contrast, the normal-normal model (**Model a**) performed substantially worse (mean difference = 40.83, SE = 7.97), indicating that heavier-tailed or skewed measurement error is needed. Because **Model d** adds an extra skewness parameter with only marginal gains, we selected the normal-t specification (**Model b**) as the final model for parsimony.

We fitted this final hierarchical measurement-error model (**Model b**) using a random sample of 100,000 donation visits, drawing four chains of 2000 warm-up and 2000 sampling iterations (8000 post-warmup draws in total). Prior specification for the model is same as for the model used in cross-validation process (table C2).

5.5 Posterior inference in real data

Trace plots of the MCMC indicated good convergences (fig. B4). Posterior estimates showed clear sex-specific differences in the population mean and variability of true Hb (table 4). The posterior mean for the true underlying Hb was 15.74 g/dL for males and 13.82 g/dL for females, each with narrow 95% posterior intervals. The estimated population variance was higher in males (1.63 (g/dL)^2 , 95% CrI: 1.60–1.67) than in females (1.13 (g/dL)^2 , 95% CrI: 1.12–1.15). Measurement error scale parameters s were similar across sexes (posterior mean 0.36 g/dL) with small degrees of freedom for both sexes. Variation due to the measurement is 22% of the total variance in females and 25% in males.

Table 4: Posterior summary statistics for model parameters, split by sex for each statistic.

Parameter	Mean		SD		Q2.5%		Q97.5%	
	Male	Female	Male	Female	Male	Female	Male	Female
μ	15.74	13.82	0.01	0.01	15.73	13.81	15.75	13.82
σ_{pop}^2	1.63	1.13	0.02	0.02	1.60	1.12	1.67	1.15
s	0.36	0.36	0.01	0.01	0.34	0.35	0.38	0.37
df	2.60	3.28	0.09	0.10	2.45	3.12	2.76	3.46

Table 5: Misclassification due to the measurement uncertainty as determined from the model posterior true Hb (T_i) and sampled measurements (x_i). The threshold c is 12.5 g/dL for females and 13 g/dL for males. FD = false deferral; FB = false bleed; PPV = positive predictive value; NPV = negative predictive value.

Sex	Strategy	FD (%)	FB (%)	1 – PPV (%)	1 – NPV (%)
Male	Single	0.9	0.4	48	0.4
	Repeat	0.2	0.6	15	0.6
Female	Single	3.3	2.5	30	2.8
	Repeat	0.7	3.7	10	4.0

Practical implications

Using posterior draws from the fitted measurement-error model, we can compute the posterior distribution of a donor’s true latent Hb (T_i) conditional on one or two observed fingerstick measurements and estimate the posterior probability that the true Hb exceeds the eligibility threshold. For example, an initial measurement of 12.8 g/dL yields a 47.3% posterior probability that the true Hb exceeds the threshold of 13 g/dL. When a second measurement of 12.4 g/dL is observed, this probability decreases to 17.4%, while a second measurement of 13.2 g/dL increases it to 59.1%. The corresponding posterior density shifts for these scenarios are shown in fig. 8.

We determined the misclassification rate due to the measurement by comparing latent true Hb (T_i) of the posterior samples with simulated measurements from the model (x_i). False deferrals are considered to be truly eligible with $T_i \geq c$, but have a measurement $x_i < c$. Vice versa, false bleeds have $T_i < c$, but $x_i \geq c$. We determined the percentage of false deferrals and false bleeds for a strategy that is based on a single measurement and for a strategy with a repeated measurement only if the prior measurement is below the threshold (see table 5). As may be expected the number of false deferrals is reduced by repeating low measurements at the cost of an increase of false bleeds.

6 Discussion

Conditionally repeating a continuous biomarker test introduces a form of sequential testing bias. Our paper illustrates how data arising from such processes can be used to isolate the contribution of the measurement process to the total variation and quantify the risk of misclassification based on one or more biomarker measurements. First, we demonstrated two frequentist methods that assume normally distributed measurement error, including a maximum likelihood method that is robust to the specific conditions under which repeated testing is performed. But, when applied to conditionally retested blood donor Hb measurements, methods unexpectedly led to inconsistent estimates of measurement variation between male and female donors (section 4.4). Second, we introduced a Bayesian hierarchical modelling framework that allows flexible distributional assumptions. Applying this framework to the blood donor Hb dataset, we found superior out-of-sample prediction using a heavy tailed distribution for the measurement error, suggesting that the normality assumptions of our frequentist approaches made them inappropriate for this application.

Routine repeat testing of Hb measurements below the threshold for donation is intended to reduce false deferrals caused by measurement error. However, in the presence of significant measurement uncertainty this practice may have unwanted consequences: it may increase the chance that donors with genuinely low Hb may still be accepted and it is not clear if this practice has the optimal effect to reduce the number of deferrals. Developing an evidence-based testing strategy requires separating measurement variability from the variability between individuals.

The current blood donation datasets that are available to us, like from Vitalant (US), present a methodological challenge, as second measurements are observed only after an initial low result. This conditional sampling violates the assumptions of standard repeat-measurement analyses that rely on unconditionally observed pairs. To address this, we developed methods that explicitly account for this selection mechanism in estimating measurement error variance.

Under the assumption that all sources of variation follow normal distributions, the repeated measurements can be represented as draws from a bivariate normal distribution. We showed that this allows us to get unbiased estimation of the correlation coefficient and, together with the total variance, can be used to decompose the variation into that present in the population and from the measurement. However, if the normality assumptions are not met, these estimates may be biased. Indeed, we found that when applying these approaches yielded different measurement error variances for males and females, which is unexpected.

To relax the distributional assumptions, we constructed a hierarchical Bayesian model that allows to specify specific distributions for both population and measurement distributions. Of the four model classes evaluated, the most parsimonious and best-fitting model assumed a normal distribution for the population and a *t*-distribution for measurement error. Applying this model to the Hb data yielded a similar scale parameter $s = 0.36 \text{ g/dL}$ for both males and females. We found that population variability is smaller in females $\widehat{\sigma_{\text{pop}}} = 1.07 \text{ g/dL}$ than in males $\widehat{\sigma_{\text{pop}}} = 1.28 \text{ g/dL}$. Population means

were also lower in females than in males ($\widehat{\mu_{\text{pop}}} = 13.82 \text{ g/dL}$ vs $\widehat{\mu_{\text{pop}}} = 15.73 \text{ g/dL}$), consistent with known sex differences in Hb levels. Note that the ratio $\sigma_{\text{pop}}/\mu_{\text{pop}}$ is quite similar between males (8.2%) and females (7.8%).

The reduced population variance in female donors may also reflect a selection effect, as individuals with very low Hb are less likely to present for donation and thus may be underrepresented in the dataset. Such a mechanism could induce skewness in the female Hb distribution. Such a model with skewness did marginally show a better fit, though not significantly (section 5.3). It would be worthwhile to explore if such a skewed distribution is appropriate.

We restricted our analysis to settings where repeated biomarkers are measured in quick succession (e.g., at a single blood donation visit) and within-person changes in biomarker levels over time may be ignored. It is straightforward to extend our Bayesian hierarchical framework to estimate within-person fluctuation as a third source of variation, which settings where repeated measurements occur on different days. Our blood donor dataset includes repeated Hb measurements on different days without intervening donations, but these constitute only approximately 0.2% of all repeated measurements. Robust estimation would require more than 100,000 samples, rendering MCMC inferences computationally infeasible. Future work could investigate alternative strategies to address the within-individual variability.

Our Bayesian method has other limitations. First, computational scalability is limited. It is well known that MCMC becomes computationally prohibitive for very large datasets, which restricts our ability to use the full set of available measurements. Our approach used many unrepeatable measurements to inform the population distribution, which is inefficient when a majority of the individuals were tested once and do not contribute directly to the estimation of measurement error. Future work could explore approximate Bayesian methods or variational inference to improve scalability, as well as targeted sub-sampling schemes that retain efficiency while reducing computational burden. Second, our analysis assumes that measurement error has a mean of 0 and is independent of the latent biomarker level. The first assumption implies that the latent biomarker level one would obtain by infinite repeated measures is the true level, ignoring the possibility of systematic overestimation or underestimation. The assumption of independent error ignores the possibility that a measurement procedure is less reliable for some biomarker levels than others. Indeed, a comparison of three point-of-care Hb devices to a "gold standard" venous Hb measurement found evidence of systematic underestimation and proportional bias [15]. Third, while our Bayesian model can estimate the misclassification risk based on one or two biomarker measurements, it only considers sex and biomarker measures at a single point in time. Future work could use additional data about the individual to refine predictions. In the case of blood donor Hb levels, considering variables like donation history, past biomarkers, and weight would likely reduce the uncertainty in posterior predictions.

Estimated measurement error and the population Hb distribution in this study can be used for a probabilistic assessment of donor eligibility. By propagating measurement uncertainty through the

model, one or two fingerstick measurements are converted into posterior probabilities that quantify confidence about a donor’s true Hb relative to the threshold (fig. 8). Our model also clarifies the value of repeat testing by indicating when a second measurement can meaningfully shift the eligibility probability versus when it adds little information, especially for borderline values near the cutoff.

In summary, this study provides a framework for disentangling population-level variation from measurement error in biomarker measurements under a selective retesting protocol. By explicitly modelling various distributional assumptions through a hierarchical Bayesian formulation, we obtained robust estimates of measurement and population variability in Hb measurements in blood donors in the US. These results can be used to inform donor eligibility in a data-driven and evidence based manner. Using our framework it is possible to determine the underlying posterior probabilities of a donors true Hb, which may be used to accurately evaluate whether a measurement should be repeated and how to interpret the repeated measurements.

Author contributions

SM conducted data analysis, methodological development and wrote the manuscript. MPJ supported the project by coordinating collaborations and contributed to the research plan. YL provided statistical expertise and contributed to writing the manuscript. WAR supervised the project, provided access to the data and contributed to the manuscript. MP also supervised the project, supported data analysis and contributed to the writing of the manuscript. WAR and MP are co-senior authors who contributed equally to this work. MPJ is deceased.

Ethics approval

This study was approved by the McGill University Research Ethics Board (reference number 22-05-018).

Acknowledgments

The authors thank the blood donors whose data enabled this study. The authors also thank collaborators Ralph Vassallo and Marjorie Bravo from Vitalant Medical Affairs and Brian Custer and Zhanna Kaidarova from Vitalant Research Institute for sharing data and providing feedback on our study.

Data and Code Availability

The analysis code is available at <https://github.com/ssm123ssm/Hb-variability---code.git>. The repository includes scripts that simulate data and apply the methods described in the manuscript.

Blood donor data were analyzed under a data sharing agreement and ethics approval that do not permit sharing of individual-level data.

Financial disclosure

This research was funded in part by the Natural Sciences and Engineering Research Council of Canada (NSERC) [funding reference number RGPIN-2023-04160, PI W. Alton Russell].

Conflict of interest

The authors declare no potential conflict of interests.

References

- [1] Aijun Niu, Xianxia Yan, Lin Wang, Yan Min, and Chengjin Hu. Utility and necessity of repeat testing of critical values in the clinical chemistry laboratory. *PLoS ONE*, 8:e80663, 11 2013.
- [2] Neda Soleimani, Amir Azadi, Mohammad Javad Esmaeli, Fatemeh Ghodsi, Reza Ghahramani, Azadeh Hafezi, Tayebeh Hosseyni, Arezoo Arabzadeh, Samira khajeh, Mahsa Farhadi, and Sahand Mohammadzadeh. Termination of repeat testing in chemical laboratories based on practice guidelines: Examining the effect of rule-based repeat testing in a transplantation center. *Journal of Analytical Methods in Chemistry*, 2021:1–7, 5 2021.
- [3] Su-Chieh Pamela Sun, JuanDavid Garcia, and Joshua A Hayden. Repeating critical hematology and coagulation values wastes resources, lengthens turnaround time, and delays clinical action. *American Journal of Clinical Pathology*, 149:247–252, 2 2018.
- [4] Elena Kulinskaya, Richard Huggins, and Samson Henry Dogo. Sequential biases in accumulating evidence. *Research Synthesis Methods*, 7:294–305, 9 2016.
- [5] John Whitehead. On the bias of maximum likelihood estimation following a sequential test. *Biometrika*, 73:573–581, 1986.
- [6] World Health Organization. *Blood Donor Selection: Guidelines on Assessing Donor Suitability for Blood Donation*. World Health Organization, 2012.
- [7] Femmeke J. Prinsze, Rosa de Groot, Tiffany C. Timmer, Saurabh Zalpuri, and Katja van den Hurk. Donation-induced iron depletion is significantly associated with low hemoglobin at subsequent donations. *Transfusion*, 61:3344–3352, 12 2021.
- [8] I Veldhuizen and E Wagenmans. *Domaine survey on donor management in Europe*, pages 148–149. 2010.

[9] Marloes L.C. Spekman, Theo G. van Tilburg, and Eva Maria Merz. Do deferred donors continue their donations? a large-scale register study on whole blood donor return in the netherlands. *Transfusion*, 59:3657–3665, 12 2019.

[10] Brian Custer, Karen S. Schlumpf, David Wright, Toby L. Simon, Susan Wilkinson, and Paul M. Ness. Donor return after temporary deferral. *Transfusion*, 51:1188–1196, 6 2011.

[11] Adrian Bruhin, Lorenz Goette, Simon Haenni, Lingqing Jiang, Alexander Markovic, Adrian Roethlisberger, Regula Buchli, and Beat M. Frey. The sting of rejection: Deferring blood donors due to low hemoglobin values reduces future returns. *Transfusion Medicine and Hemotherapy*, 47:119–128, 2020.

[12] Meaghan M. Bond and Rebecca R. Richards-Kortum. Drop-to-drop variation in the cellular components of fingerprick blood: Implications for point-of-care diagnostic development. *American Journal of Clinical Pathology*, 144:885–894, 12 2015.

[13] Laura S. Hackl, Crystal D. Karakochuk, Dora Inés Mazariegos, Kidola Jeremiah, Omar Obeid, Nirmal Ravi, Desalegn A. Ayana, Veronica Varela, Silvia Alayón, Omar Dary, and Denish Moorthy. Assessing accuracy and precision of hemoglobin determination in venous, capillary pool, and single-drop capillary blood specimens using three different hemocue® hb models: The multi-country hemoglobin measurement (heme) study. *Journal of Nutrition*, 154:2326–2334, 7 2024.

[14] David W. Killilea, Frans A. Kuypers, Sandra K. Larkin, and Kathleen Schultz. Blood draw site and analytic device influence hemoglobin measurements. *PLoS ONE*, 17, 11 2022.

[15] Steven Bell, Michael Sweeting, Anna Ramond, Ryan Chung, Stephen Kaptoge, Matthew Walker, Thomas Bolton, Jennifer Sambrook, Carmel Moore, Amy McMahon, Sarah Fahle, Donna Cullen, Susan Mehenny, Angela M. Wood, Jane Armitage, Willem H. Ouwehand, Gail Miflin, David J. Roberts, John Danesh, and Emanuele Di Angelantonio. Comparison of four methods to measure haemoglobin concentrations in whole blood donors (compare): A diagnostic accuracy study. *Transfusion Medicine*, 31:94–103, 4 2021.

[16] Mart P. Janssen. Why the majority of on-site repeat donor deferrals are completely unwarranted.... *Transfusion*, 62:2068–2075, 10 2022.

[17] Saurabh Zalpuri, Bas Romeijn, Elias Allara, Mindy Goldman, Hany Kamel, Jed Gorlin, Ralph Vassallo, Yves Grégoire, Naoko Goto, Peter Flanagan, Joanna Speedy, Andreas Buser, Jose Mauro Kutner, Karin Magnussen, Johanna Castrén, Liz Culler, Harry Sussmann, Femmeke J. Prinsze, Kevin Belanger, Veerle Compernolle, Pierre Tiberghien, Jose Manuel Cardenas, Manish J. Gandhi, Kamille A. West, Cheuk-Kwong Lee, Sian James, Deanne Wells, Laurie J. Sutor, Silvano Wendel, Matthew Coleman, Axel Seltsam, Kimberly Roden, Whitney R. Steele, Milos Bohonek, Ramir Alcantara, Emanuele Di Angelantonio, and Katja van den Hurk. Variations in hemoglobin measurement and eligibility criteria across blood donation services are associated with differing low-hemoglobin deferral rates: a best collaborative study. *Transfusion*, 60:544–552, 3 2020.

- [18] Ryan K. Chung, Angela M. Wood, and Michael J. Sweeting. Biases incurred from nonrandom repeat testing of haemoglobin levels in blood donors: Selective testing and its implications. *Biometrical Journal*, 61:454–466, 3 2019.
- [19] Mart Pothast, Katja van den Hurk, and Mart P. Janssen. Modeling the effect of conditionally repeating hemoglobin measurements prior to blood donation. *Transfusion*, 65:1395–1399, 8 2025.
- [20] Federica Braga and Mauro Panteghini. Generation of data on within-subject biological variation in laboratory medicine: An update. *Critical Reviews in Clinical Laboratory Sciences*, 53:313–325, 9 2016.
- [21] Norman Lloyd. Johnson, Samuel. Kotz, and N.. Balakrishnan. *Continuous univariate distributions*. Wiley, 1994.
- [22] Paul Gustafson. *Measurement error and misclassification in statistics and epidemiology: impacts and Bayesian adjustments*. Chapman and Hall/CRC, 2003.
- [23] Sander Greenland. Multiple-bias modelling for analysis of observational data. *Journal of the Royal Statistical Society Series A: Statistics in Society*, 168(2):267–306, 2005.
- [24] Yu Luo, David A Stephens, and David L Buckeridge. Estimating prevalence using indirect information and bayesian evidence synthesis. *Canadian Journal of Statistics*, 46(4):673–689, 2018.
- [25] HK Walker, WD Hall, and JW Hurst, editors. *Clinical Methods: The History, Physical, and Laboratory Examinations, Chapter 151*. Butterworths, 3 edition, 1990.
- [26] Aki Vehtari, Andrew Gelman, and Jonah Gabry. Practical bayesian model evaluation using leave-one-out cross-validation and waic. *Statistics and Computing*, 27:1413–1432, 9 2017.

A Blood donor data selection

Our applied example uses data from Vitalant, a large blood operator in the United States. The full dataset contains hemoglobin measurements from donor visits between January 1, 2017 and October 31, 2022 and is comprised of 2,582,402 unique donors with 9,099,136 visits recorded in the database, of which 6,528,084 had a pre-donation fingerstick Hb measurement.

The majority of the visits were intended for whole blood donation visits, comprising 68% of the total. Double red-cell donation visits accounted for 10% of visits, while plasma and platelet donation visits represented 12% and 10% of visits did not result in a successful donation for various reasons. The sex-specific hemoglobin threshold for donation eligibility was 13 g/dL for males and 12.5 g/dL for females. If the initial pre-donation fingerstick Hb fell below this threshold, a second fingerstick Hb measurement was performed and recorded in the database. The majority of visits (90%) with a Hb value below the threshold for the first test underwent a second test the same day. The data selection flow chart is shown in fig. A1.

B Additional figures

C Additional tables

Table C1: Data-generating parameter values used in the simulation study. Latent parameters specify the distribution of the true latent quantity; measurement parameters govern observation noise. Vectors give sex-specific values in the order (male, female). For model c, $\sigma_{\text{meas},1}$ and $\sigma_{\text{meas},2}$ are the mixture component scales and π is the mixture weight; for models b and d, df is the Student- t degrees of freedom.

Model	Latent distribution parameters	Measurement parameters
Model a	$\mu = (14.8, 13.8)$ $\sigma_{\text{pop}} = (0.55, 0.60)$	$\sigma_{\text{meas}} = (0.55, 0.55)$
Model b	$\mu = (14.8, 13.8)$ $\sigma_{\text{pop}} = (0.55, 0.60)$	$\sigma_{\text{meas}} = (0.55, 0.55)$ $\text{df} = (5, 5)$
Model c	$\mu = (14.8, 13.8)$ $\sigma_{\text{pop}} = (0.55, 0.60)$	$\sigma_{\text{meas},1} = (0.45, 0.45)$ $\sigma_{\text{meas},2} = (2.0, 2.2)$ $\pi = 0.80$
Model d	$\mu_{\text{loc}} = (14.8, 13.8)$ $\mu_{\text{scale}} = (0.55, 0.60)$ $\mu_{\text{skew}} = (5, -5)$	$\sigma_{\text{meas}} = (0.55, 0.55)$ $\text{df} = (5, 5)$

Table C2: Priors used for real-data models (sex-specific parameters). Parameter bounds (caps) follow the model definitions: $\sigma_{\text{pop}}, \sigma_{\text{meas}} \in [0.2, 20]$; $\text{df} \in [2, 30]$; for the mixture model $\sigma_{\text{meas},1}, \sigma_{\text{meas},2} \in [0.2, 2]$ and $\pi \in [0, 1]$; for the skew model $\mu_{\text{skew}} \in [-5, 5]$, $\sigma_{\text{meas}} \in [0.2, 2]$, and $\text{df} \in [2, 30]$.

Model	Priors
Model a (Normal–normal)	$\mu \sim \mathcal{N}(15, 2)$; $\sigma_{\text{pop}} \sim \mathcal{N}(0, 2)$; $\sigma_{\text{meas}} \sim \mathcal{N}(0, 2)$
Model b (Normal–t)	$\mu \sim \mathcal{N}(15, 2)$; $\sigma_{\text{pop}} \sim \mathcal{N}(0, 2)$; $\sigma_{\text{meas}} \sim \mathcal{N}(0, 2)$; $\text{df} \sim \text{Gamma}(2, 0.1)$
Model c (Mixture)	$\mu \sim \mathcal{N}(15, 2)$; $\sigma_{\text{pop}} \sim \mathcal{N}(0, 2)$; $\sigma_{\text{meas},1} \sim \mathcal{N}(0, 2)$; $\sigma_{\text{meas},2} \sim \mathcal{N}(2, 2)$; $\pi \sim \text{Beta}(2, 2)$
Model d (Skew–t)	$\mu_{\text{loc}} \sim \mathcal{N}(15, 2)$; $\mu_{\text{scale}} \sim \mathcal{N}(1, 2)$; $\mu_{\text{skew}} \sim \mathcal{N}(0, 2)$; $\sigma_{\text{meas}} \sim \mathcal{N}(1, 2)$; $\text{df} \sim \text{Gamma}(2, 0.1)$

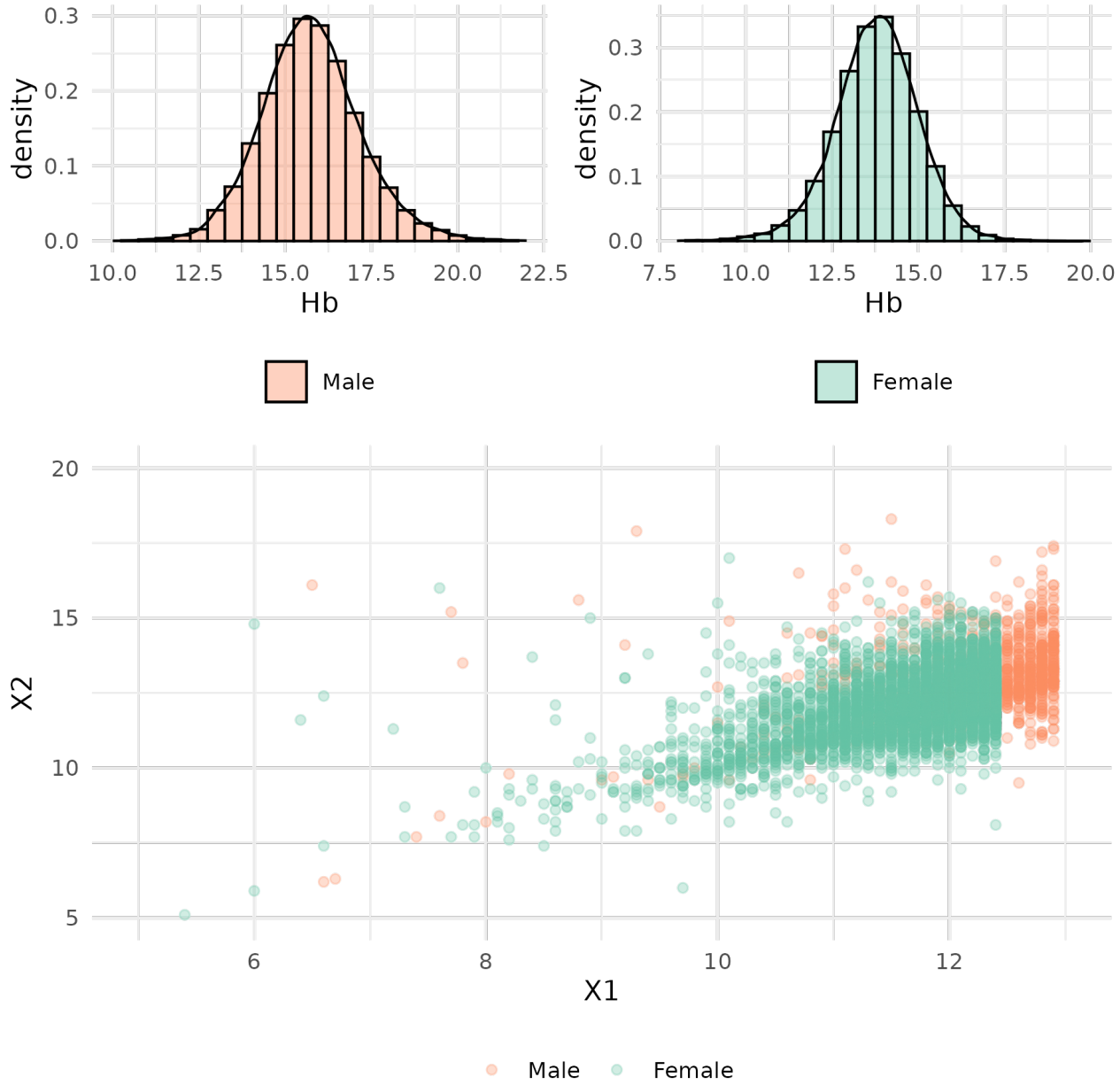


Figure 1: (Top:) Distribution of the first Hb measurement of males and females at all blood donor visits. (Bottom:) scatterplot of the first (X1) and the repeat (X2) Hb measurement among the subset of donors with two measurements at the same visit.

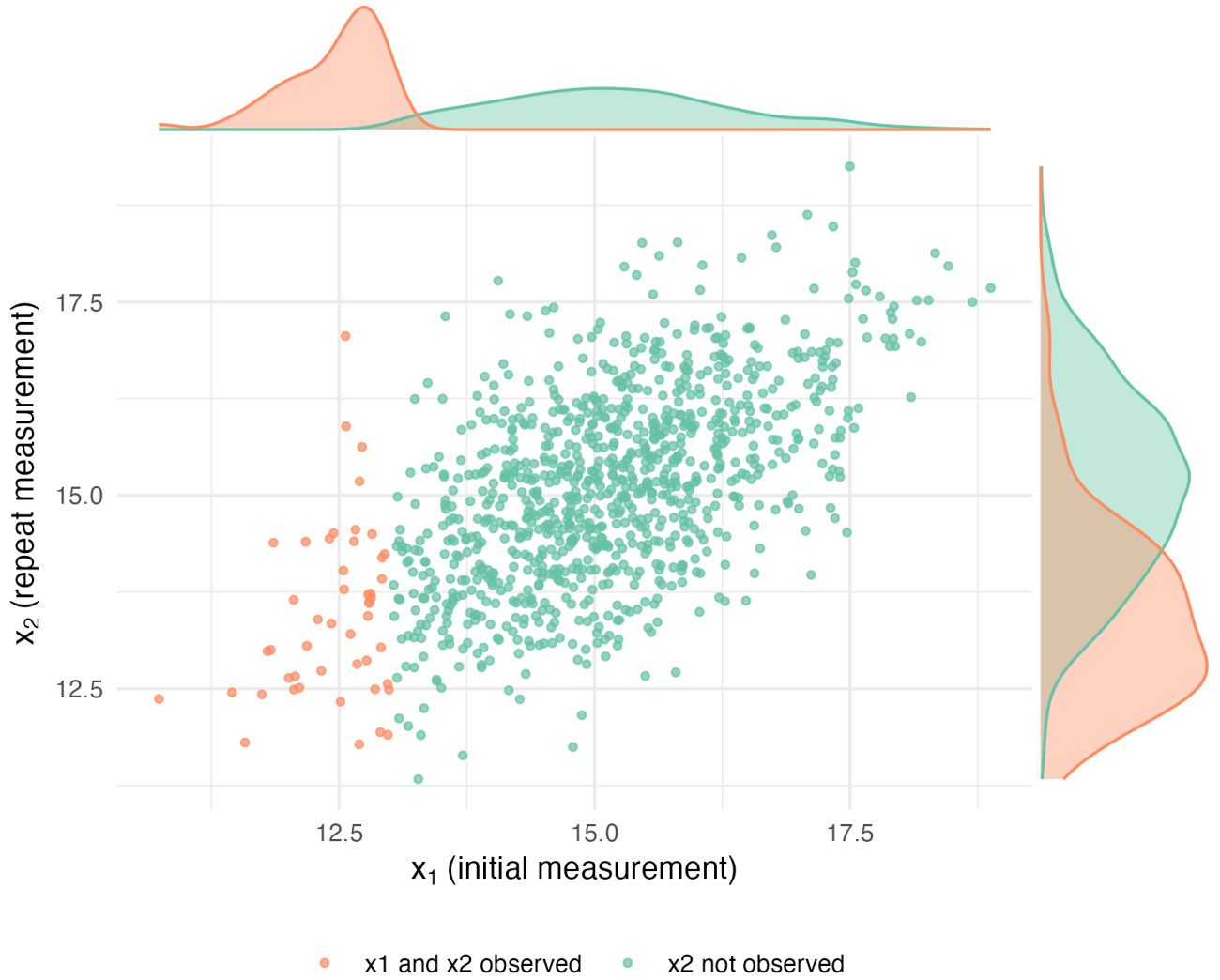


Figure 2: Scatter plot of the initial and repeat measurement of 1000 simulated conditionally repeated measurements. Density plots show the marginal distribution of x_1 and x_2 when pairs are observed for all individuals (green) and when x_2 is only observed when x_1 falling falls below $c = 13$ g/dL (orange).

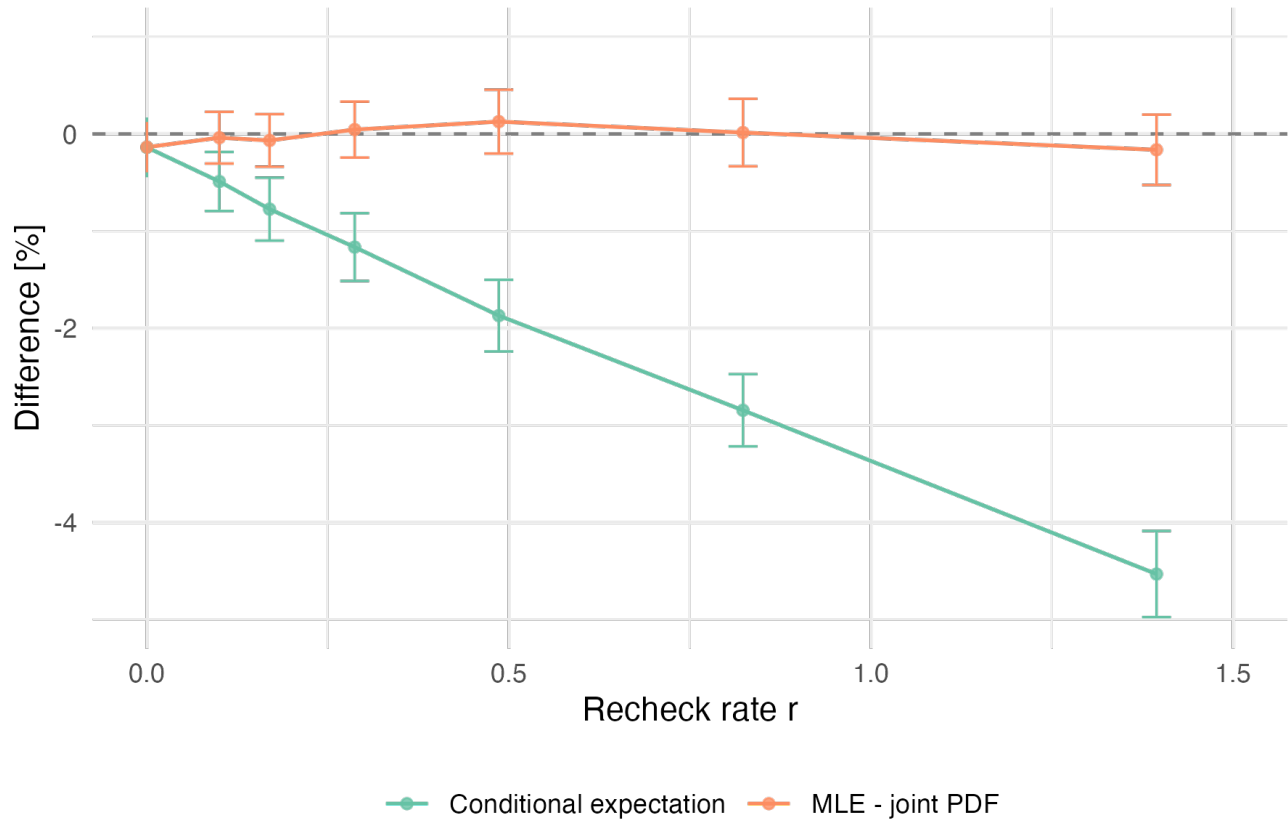


Figure 3: Difference between estimated $\hat{\sigma}_{\text{meas}}$ and simulated $\sigma_{\text{meas}} = 0.8 \text{ g/dL}$. Shown is the mean with 95% CI of 200 repeats of simulated datasets with recheck probability parameter r from eq. (23).

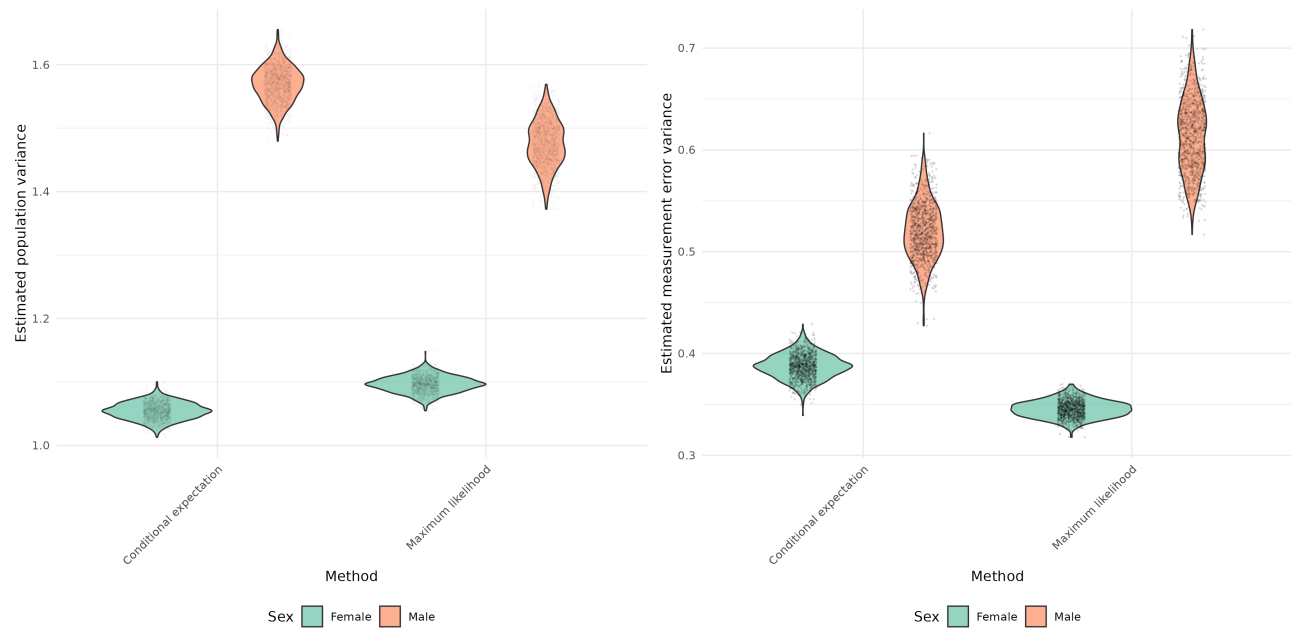


Figure 4: Violin plots depicting the distribution of bootstrapped estimates for population variance and measurement error variance using the conditional expectation method and maximum likelihood method, stratified by sex

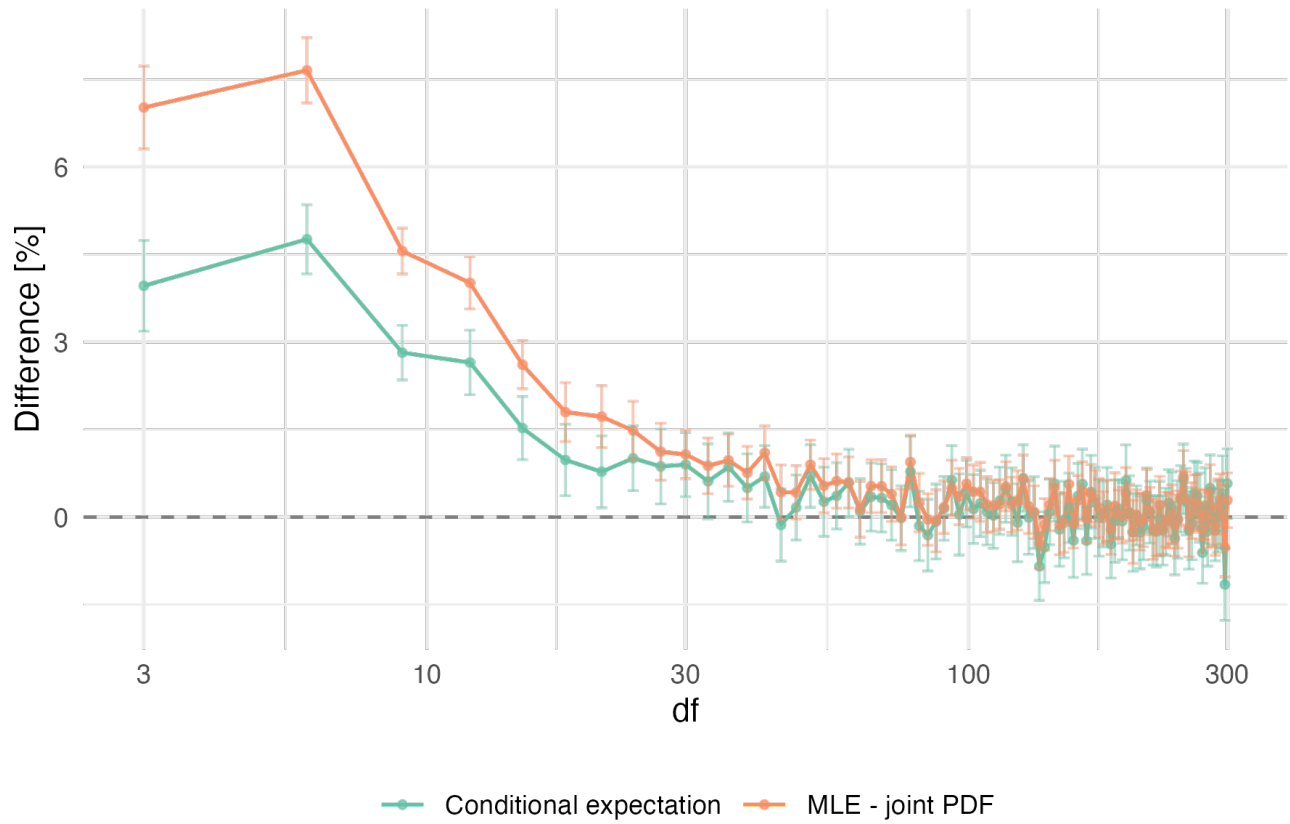
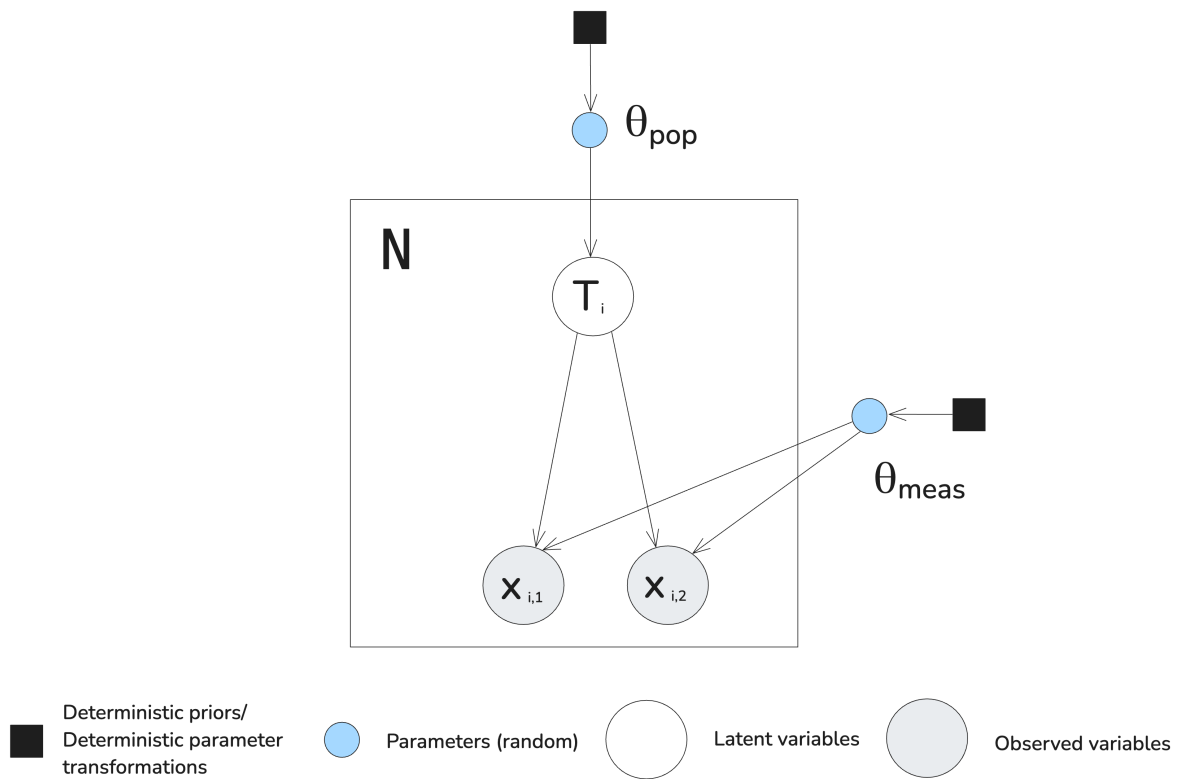


Figure 5: Percent difference between the estimated measurement error variance and the true variance (accounting for degrees of freedom) for conditional expectation and maximum likelihood methods under truncation with a t distributed error measurement. Points show mean bias across 100 simulations with 95% confidence intervals, plotted against the degrees of freedom (df) on a log scale.



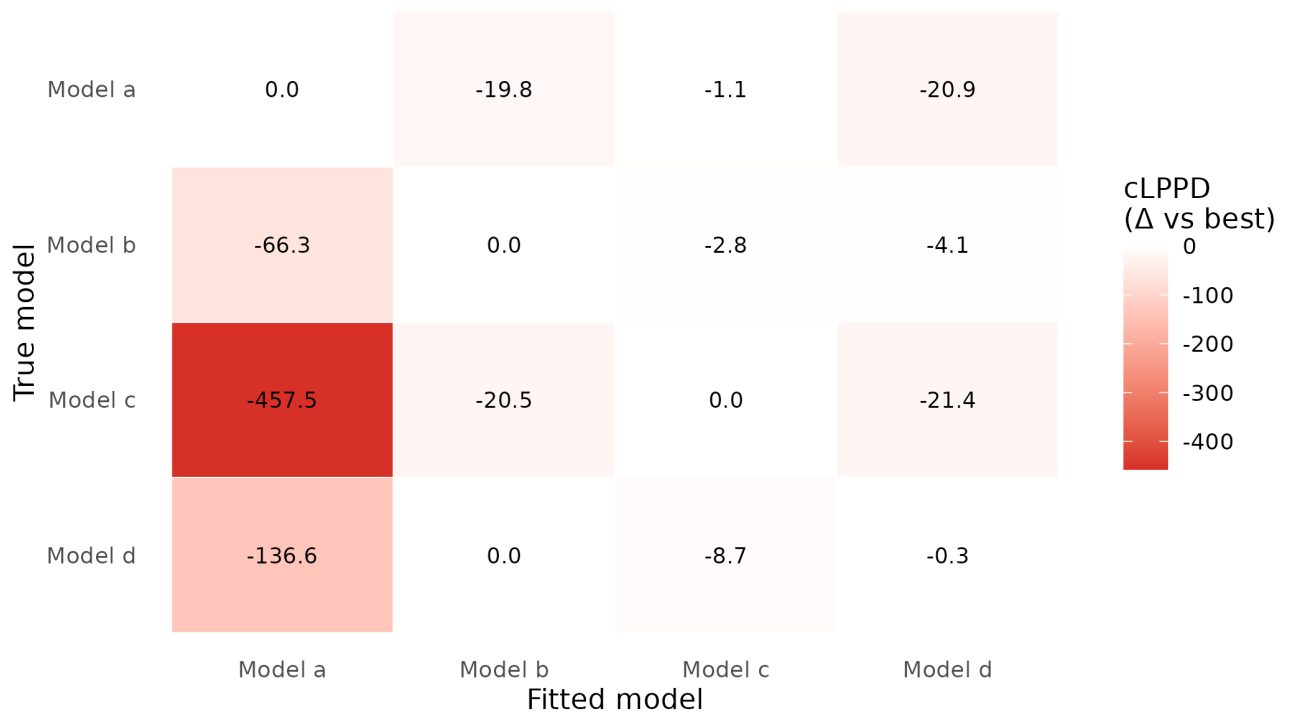


Figure 7: Delta cLPPD heatmap from 5-fold CV on synthetic datasets. Each tile shows the total cLPPD for a fitted model minus the best cLPPD within the same true-model dataset (higher is better, 0 indicates the winner). Negative values indicate worse predictive performance relative to the best model for that dataset.

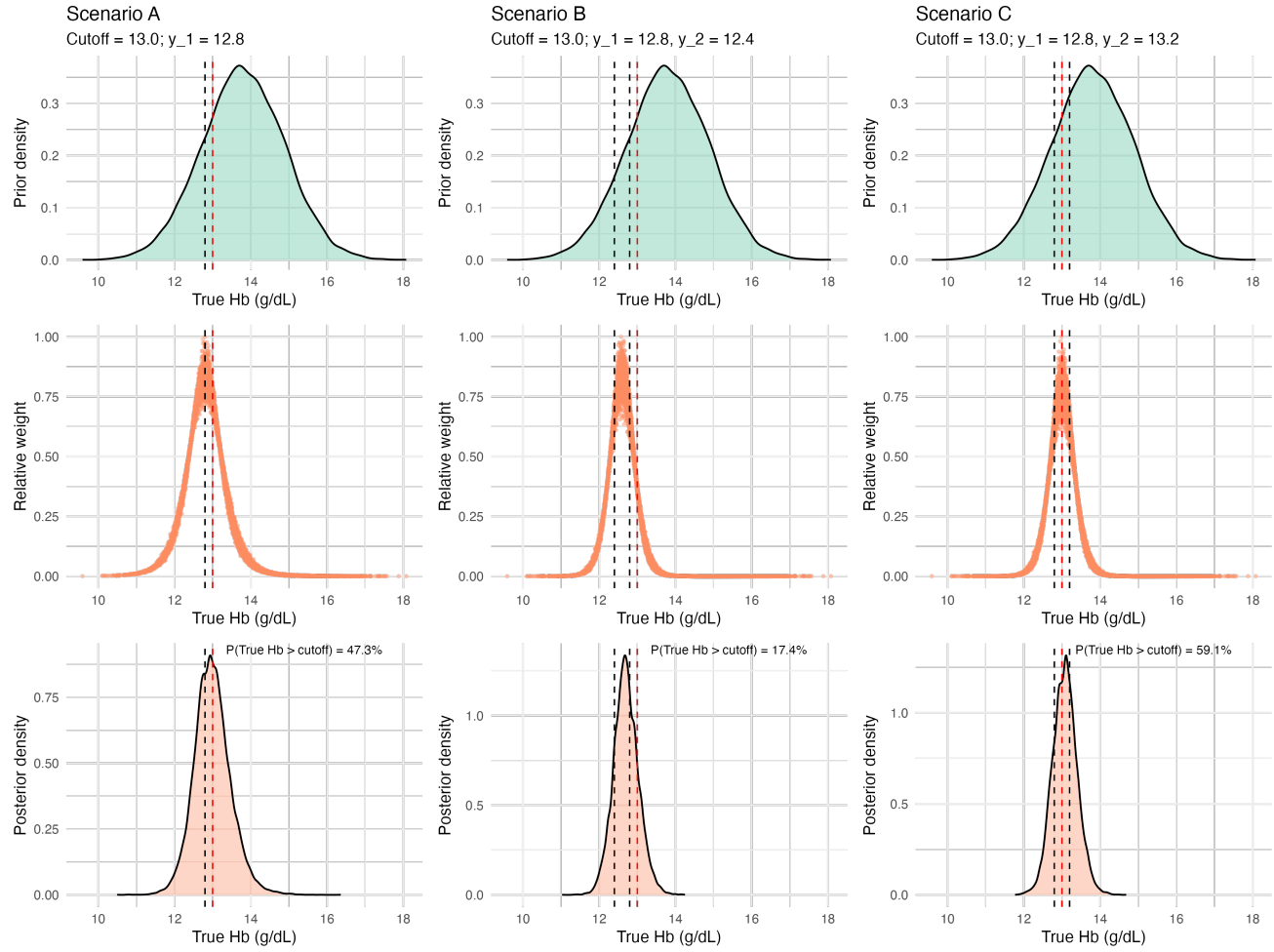


Figure 8: Prior, likelihood, and posterior for three scenarios (columns A - C) with a 13 g/dL cutoff and initial Hb of 12.8 g/dL. Scenario A uses one measurement; B adds 12.4 g/dL; C adds 13.2 g/dL. Red dashed lines mark the cutoff, black dashed lines the observed measurements.

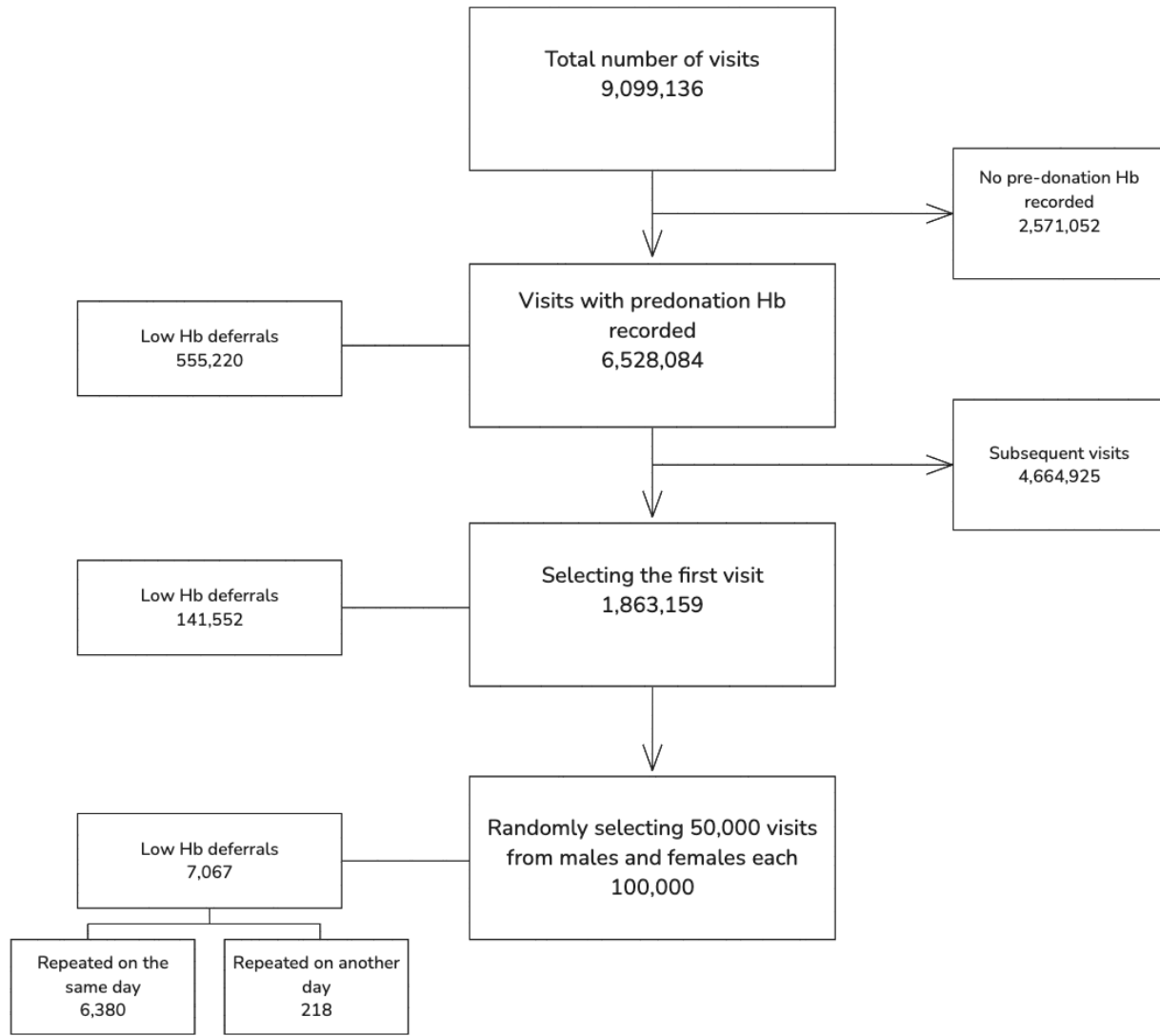


Figure A1: Flow chart of selecting donation visits.

Bootstrap CI for numerical bias vs theoretical bias

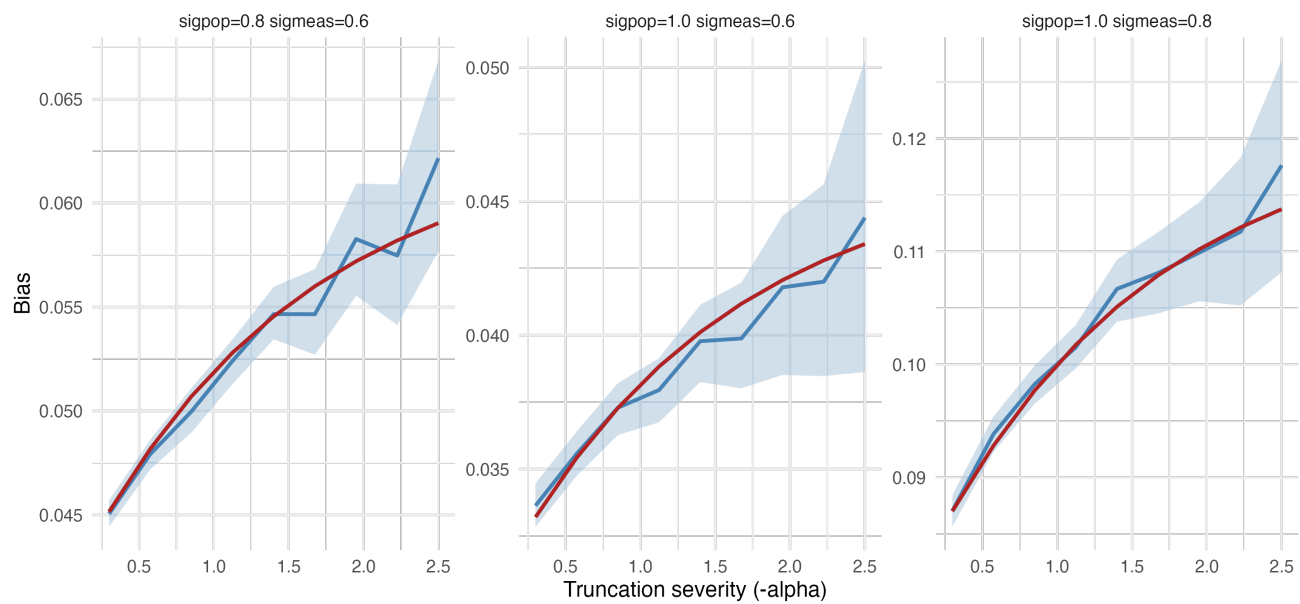


Figure B1: Bias under conditional repeat measurements across parameter sets. Lines show the theoretical bias as a function of truncation severity, and shaded bands show bootstrap 95% confidence intervals for the numerical bias from simulations; stronger truncation yields larger downward bias.

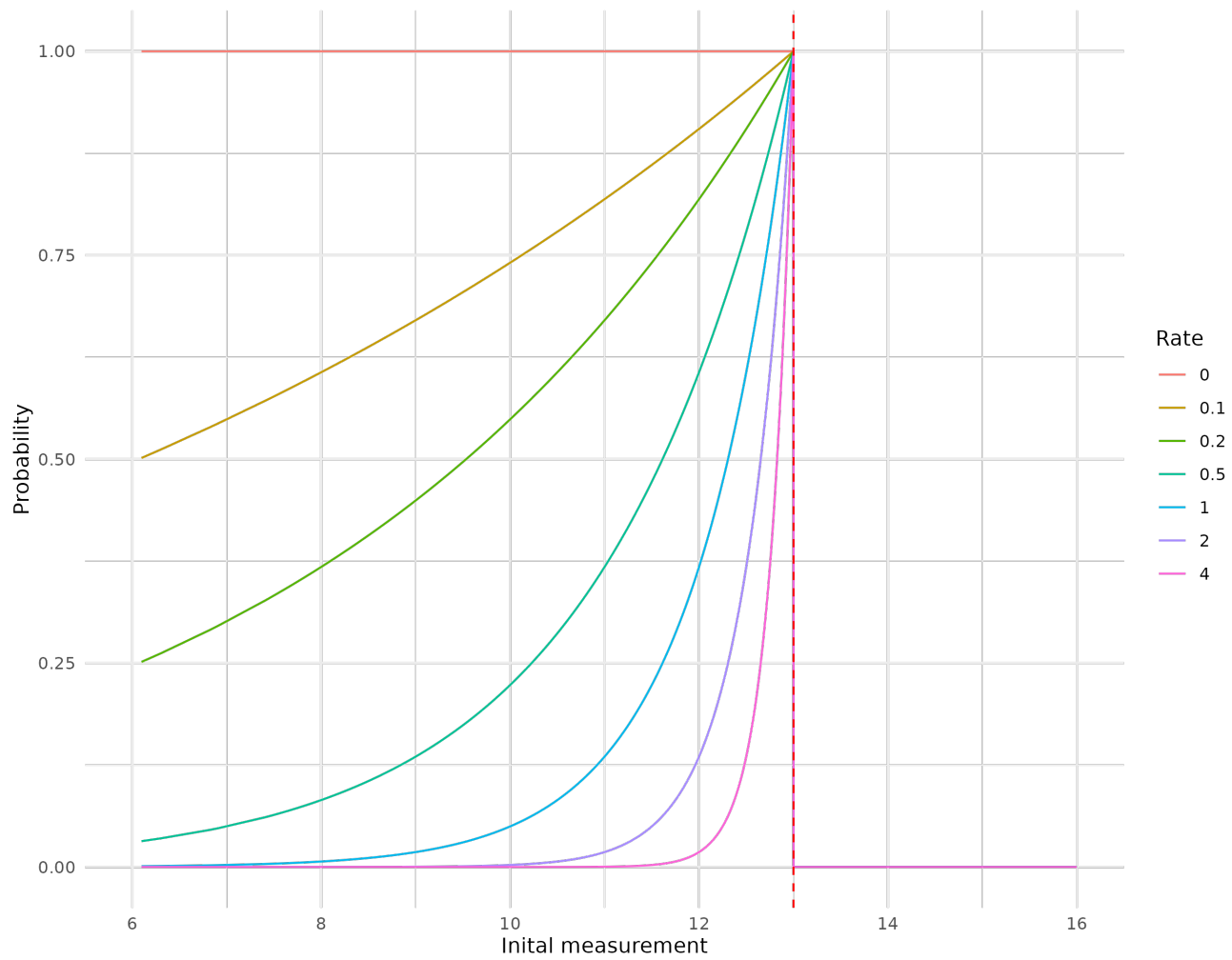


Figure B2: Simulating additional dependencies for repeating a measurement. Each colored line corresponds to the probability of performing a repeat measurement based on the initial measurement.

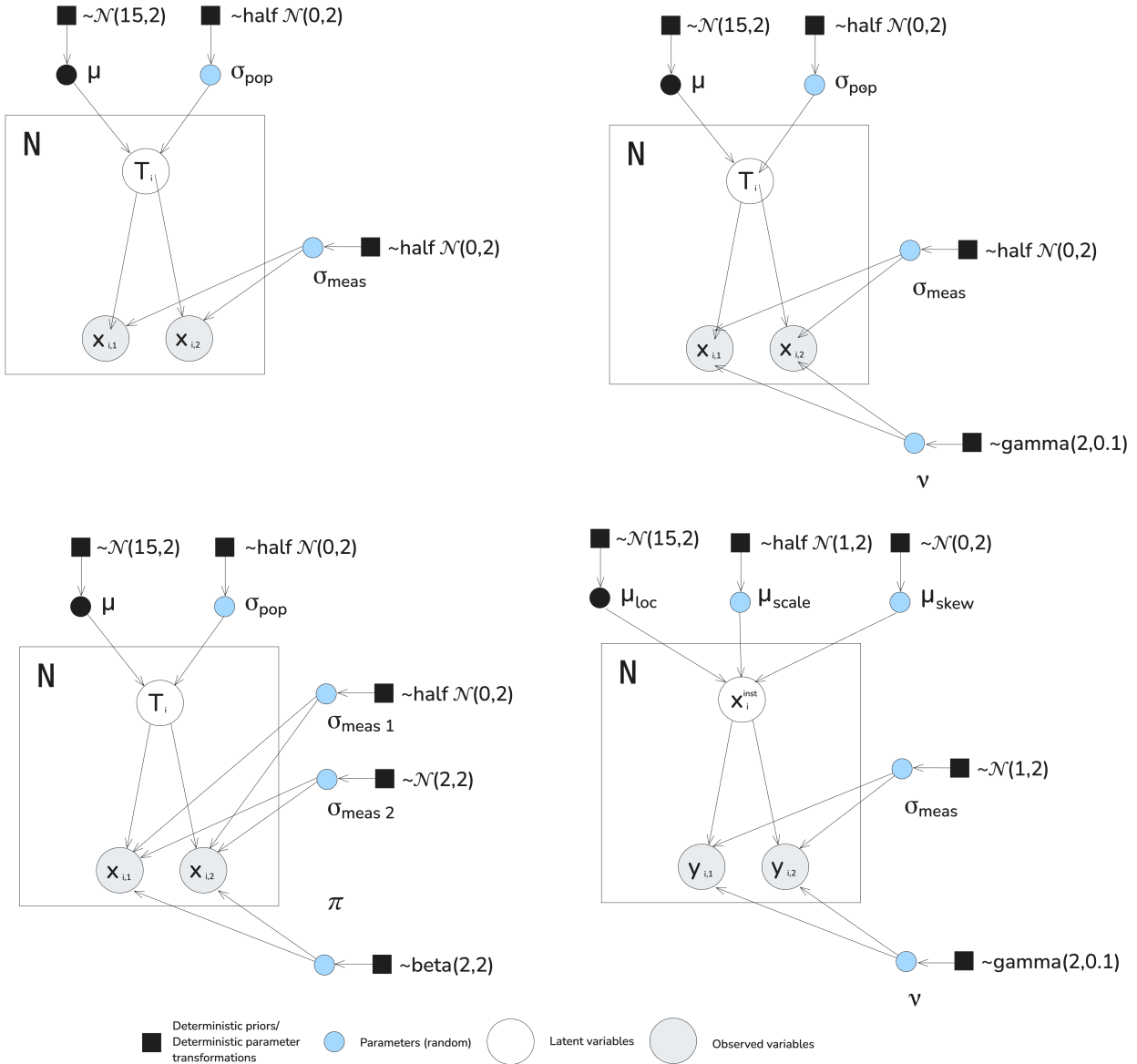


Figure B3: Distributional assumptions tested

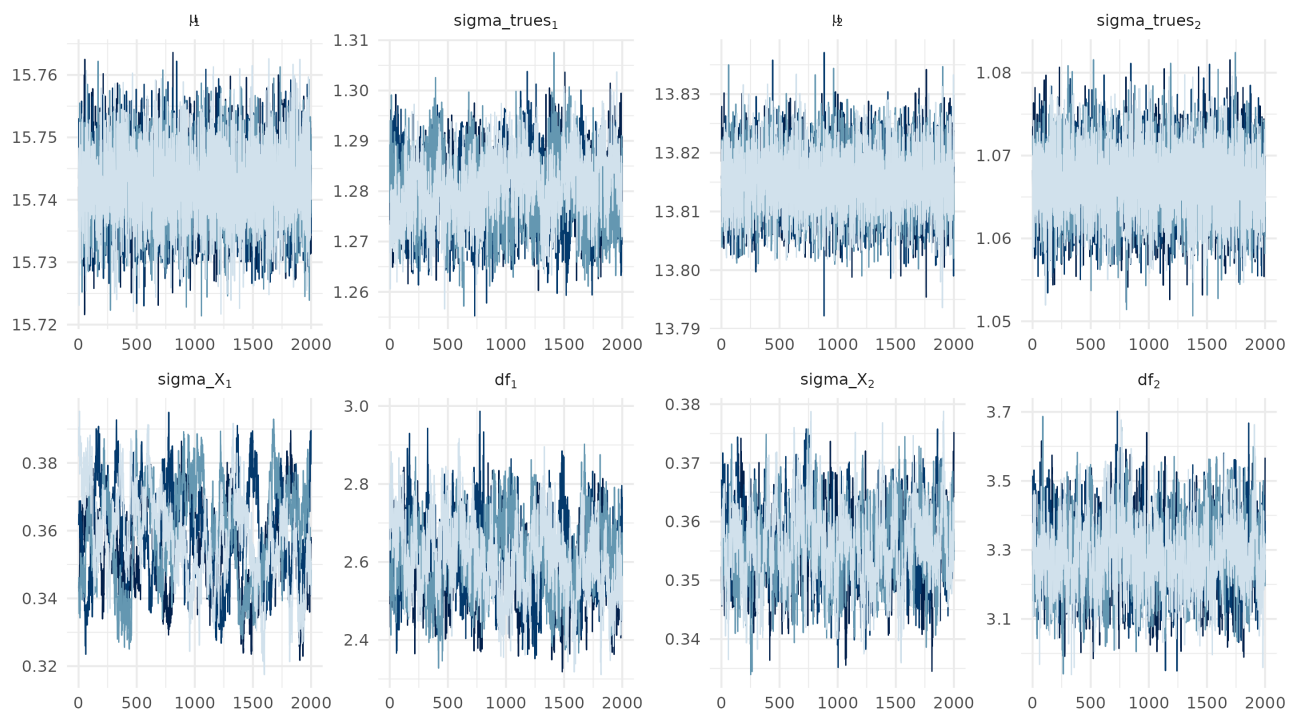


Figure B4: Traceplots of the model for the global parameters for males and females. The plots show the parameter estimates of the four chains across the post warm-up iterations.

Table C3: Parameter recovery summary for data simulation under each generation process (posterior mean and 95% credible interval).

Model	Parameter	Mean	2.5%	97.5%
Model a	μ_1	14.825	14.780	14.870
	μ_2	13.764	13.716	13.812
	$\sigma_{\text{meas},1}$	0.542	0.517	0.569
	$\sigma_{\text{meas},2}$	0.557	0.530	0.587
	$\sigma_{\text{pop},1}$	0.601	0.561	0.642
	$\sigma_{\text{pop},2}$	0.624	0.581	0.669
Model b	df_1	5.711	4.234	7.617
	df_2	6.038	4.445	7.771
	μ_1	14.783	14.736	14.832
	μ_2	13.802	13.753	13.851
	$\sigma_{\text{meas},1}$	0.542	0.497	0.585
	$\sigma_{\text{meas},2}$	0.564	0.518	0.606
	$\sigma_{\text{pop},1}$	0.566	0.519	0.614
	$\sigma_{\text{pop},2}$	0.606	0.557	0.655
	π	0.739	0.471	0.838
	μ_1	14.821	14.774	14.869
Model c	μ_2	13.829	13.777	13.880
	$\sigma_{\text{meas},1,1}$	0.416	0.276	0.487
	$\sigma_{\text{meas},1,2}$	0.719	0.426	1.565
	$\sigma_{\text{meas},2,1}$	1.869	1.340	2.214
	$\sigma_{\text{meas},2,2}$	1.732	0.264	2.433
	$\sigma_{\text{pop},1}$	0.545	0.481	0.597
	$\sigma_{\text{pop},2}$	0.615	0.551	0.669
	df_1	5.611	4.290	7.301
	df_2	5.949	4.512	7.612
	$\mu_{\text{loc},1}$	14.864	14.773	14.973
Model d	$\mu_{\text{loc},2}$	13.839	13.728	13.923
	$\mu_{\text{scale},1}$	0.479	0.375	0.576
	$\mu_{\text{scale},2}$	0.658	0.559	0.750
	$\mu_{\text{skew},1}$	4.849	1.247	11.590
	$\mu_{\text{skew},2}$	-5.638	-11.713	-2.122
	$\sigma_{\text{meas},1}$	0.568	0.524	0.609
	$\sigma_{\text{meas},2}$	0.580	0.538	0.622

Table C4: Total cLPPD by true model and fitted model (5-fold CV).

True model	Fitted model	Total cLPPD
Model a	Model a	-4012.0
	Model b	-4031.9
	Model c	-4013.2
	Model d	-4032.9
Model b	Model a	-4402.6
	Model b	-4336.3
	Model c	-4339.1
	Model d	-4340.4
Model c	Model a	-5346.9
	Model b	-4910.0
	Model c	-4889.4
	Model d	-4910.8
Model d	Model a	-4173.6
	Model b	-4037.0
	Model c	-4045.7
	Model d	-4037.3

Table C5: Per-fold computed LPPD (cLPPD) for the four candidate models. Mean and standard error (SE) are computed across the five folds. Each row lists the per-fold cLPPD (folds 1 - 5) followed by the across-fold mean and standard error (SE). Larger (less negative) cLPPD indicates better predictive performance. The maximum cLPPD in each column is bolded.

Model	Fold 1	Fold 2	Fold 3	Fold 4	Fold 5	Mean	SE
Model a (Normal–normal)	-11298.27	-11335.27	-11338.68	-11229.12	-11122.52	-11264.77	40.66
Model b (Normal–t)	-11251.73	-11313.39	-11309.15	-11151.97	-11105.21	-11226.29	42.00
Model c (Mixture)	-11243.57	-11310.46	-11305.82	-11199.73	-11098.05	-11231.53	39.19
Model d (Skew–t)	-11242.39	-11306.80	-11310.03	-11164.87	-11095.61	-11223.94	41.58